DESY 65/10
Oktober 1965
Theorie

PAIR PRODUCTION AND HEAVY ELECTRON

by

F. Gutbrod and D. Schildknecht

DEUTSCHES ELEKTRONEN-SYNCHROTRON DESY

DEUTSCHES ELEKTRONEN-SYNCHROTRON DESY, HAMBURG

PAIR PRODUCTION AND HEAVY ELECTRON

by F. Gutbrod and D. Schildknecht

Production of electron positron pairs is analysed with the hypothesis of the heavy electron e*. A rough agreement between theory and experiment is found if the coupling constant is suitably chosen as a function of the mass m* of the e*. Comparison with upper limits for this coupling constant taken from inelastic electron proton scattering indicates that a heavy electron with m* between 12o MeV and 1 GeV cannot explain observed deviations from pure quantum electrodynamics.

1. Introduction

In connection with tests of quantum electrodynamics at small distances Low has recently suggested [1] to search for electron photon resonances and remarked that the deviation from simple electrodynamics in electron positron pair production found by the authors of ref. 2 might be caused by such an electron photon resonance e*. We give an estimate of the coupling strength λ between e,e* and γ (or equivalent the width of the e*) which is necessary to explain the deviations mentioned. λ of course depends on the mass m* of the heavy electron which is varied between 0,12 and 1,5 GeV. Recent experiments on electron proton scattering [3,4] gave upper limits of λ in the mass interval $0{,}12 \leq m^* \leq 1{,}0$ GeV. It turns out that λ needed to fit the pair production experiment lies considerably above these limits.

Specifically, in section 2, we thus give the cross section for pair production including the virtual e*, and, in section 3, the cross section for production of the e* in electron proton scattering. In section 4 pair production is discussed numerically and conclusions are drawn.

2. Cross Section for Pair Production

By Lorentz invariance and electromagnetic current conservation the interaction Lagrangian for the interaction of the heavy electron with the electron and the electromagnetic field $F_{\mu\nu}$ is given by [1†]

$$L_{int} = \lambda \frac{e}{m^*} \left(\bar{\psi}_{e^*} \sigma^{\mu\nu} \psi_e F_{\mu\nu} + h.c. \right). \qquad (1)$$

---

†) The metric $g^{00}=1$, $g^{11}= g^{22}= g^{33} = -1$ is used and $\sigma^{\mu\nu} = \frac{1}{2i}(\gamma^\mu\gamma^\nu - \gamma^\nu\gamma^\mu)$.

The principal features of the influence of the e* on the pair production cross section may be seen by considering pair production by an external field, which will be done subsequently. The Feynman diagrams ‡) to be evaluated are shown in Fig. 1. The cross section for pair production by unpolarized photons is then given by

$$\frac{d^3\sigma}{d\Omega_+ d\Omega_- dE_+} = -A\sum_\lambda tr\left\{\Lambda_+(p_-)\left(L_1^{(\lambda)}+L_2^{(\lambda)}+S_1^{(\lambda)}+S_2^{(\lambda)}\right)\Lambda_-(p_+)\left(L_{1R}^{(\lambda)}+L_{2R}^{(\lambda)}+S_{1R}^{(\lambda)}+S_{2R}^{(\lambda)}\right)\right\} \quad (2)$$

In this expression A is a kinematical factor

$$A = \frac{2\alpha^3 Z^2 m^2}{(2\pi)^2}\,\frac{|\vec{p}_+|\,|\vec{p}_-|}{q^4\,k^0}, \quad (3)$$

p_-, p_+ and k denote the fourmomentum of the electron, positron and photon respectively, $q = p_+ + p_- - k$, and $\Lambda_\pm(p)$ are the usual projection operators

$$\Lambda_\pm(p) = \frac{1}{2m}\left(\pm \not{p} + m\right) \quad (4)$$

For $L_{1,2}^{(\lambda)}$ and $S_{1,2}^{(\lambda)}$ we have

$$\begin{aligned} L_1^{(\lambda)} &= -\not{n}\,\frac{\not{k}-\not{p}_+ + m}{(k-p_+)^2 - m^2}\,\not{e}^{(\lambda)} \\ L_2^{(\lambda)} &= -\not{e}^{(\lambda)}\,\frac{\not{p}_- - \not{k} + m}{(p_- - k)^2 - m^2}\,\not{n} \\ S_1^{(\lambda)} &= \left(\frac{2\lambda}{m^*}\right)^2 \sigma^{\mu\nu} n_\mu q_\nu\,\frac{\not{k}-\not{p}_+ + m^*}{(k-p_+)^2 - m^{*2}}\,\sigma^{\alpha\beta} e_\alpha^{(\lambda)} k_\beta \\ S_2^{(\lambda)} &= \left(\frac{2\lambda}{m^*}\right)^2 \sigma^{\alpha\beta} e_\alpha^{(\lambda)} k_\beta\,\frac{\not{p}_- - \not{k} + m^*}{(p_- - k)^2 - m^{*2}}\,\sigma^{\mu\nu} n_\mu q_\nu \end{aligned} \quad (5)$$

where n denotes the fourvector of the external potential with

$$n^2 = 1\;; \quad nq = 0\,, \quad (6)$$

----

‡) The exchange of a particle with magnetic coupling leads to a cross section, which does not decrease as the virtual mass of the e* increases. The corresponding unitarity difficulties should be removed by introducing a cutoff, which will be neglected in our treatment. We hope therefore, that we can regard our values of λ, obtained from comparison with experiment, as lower limits.

and $e^{(\lambda)}$ are the polarisation vectors of the incoming photon with

$$e^{(\lambda)} \cdot k = 0 . \tag{7}$$

$L_{1R}^{(\lambda)}$ can be obtained from $L_1^{(\lambda)}$ by writing all γ's in the reverse order. The trace in (2) has the form $n_\mu n_\nu T^{\mu\nu}$ where the tensor $T^{\mu\nu}$ is a linear combination of $g^{\mu\nu}$ and the tensors formed from k^μ, p_+^μ, p_-^μ and q^μ. Because of four momentum conservation and because of $n \cdot q = 0$, $T^{\mu\nu}$ may be written as a linear combination of $g^{\mu\nu}$ and the tensors formed from two of the vectors k^μ, p_+^μ, and p_-^μ . We shall choose k^μ and p_-^μ . The coefficients depend on three linearly independent combinations of the four vectors mentioned and will subsequently be chosen to be q^2, kp_+ and kp_-.

Only 6 of the 16 traces appearing in (2) have to be calculated explicitly. We first note that from well known properties of traces of γ-matrices one has

$$\begin{aligned} &tr\left\{\Lambda_+(p_-)\left(L_1^{(\lambda)}+L_2^{(\lambda)}\right)\Lambda_-(p_+)\left(S_{1R}^{(\lambda)}+S_{2R}^{(\lambda)}\right)\right\} = \\ &= tr\left\{\left(S_1^{(\lambda)}+S_2^{(\lambda)}\right)\Lambda_-(p_+)\left(L_{1R}^{(\lambda)}+L_{2R}^{(\lambda)}\right)\Lambda_+(p_-)\right\} \end{aligned} \tag{8}$$

which reduces the number of traces to 12. Only half of them have to be evaluated explicitly as the remaining ones may be obtained by performing the substitution

$$\begin{aligned} p_- &\rightarrow -p_+ \\ p_+ &\rightarrow -p_- \\ k &\rightarrow -k \\ (q &\rightarrow -q) \end{aligned} \tag{9}$$

i.e., we finally have

$$\begin{aligned} &\sum_\lambda tr\left\{\Lambda_+(p_-)\left(L_1^{(\lambda)}+L_2^{(\lambda)}+S_1^{(\lambda)}+S_2^{(\lambda)}\right)\Lambda_-(p_+)\left(L_{1R}^{(\lambda)}+L_{2R}^{(\lambda)}+S_{1R}^{(\lambda)}+S_{2R}^{(\lambda)}\right)\right\} = \\ &= \Big[\sum_\lambda tr\left\{\Lambda_+(p_-)L_1^{(\lambda)}\Lambda_-(p_+)\left(L_{1R}^{(\lambda)}+L_{2R}^{(\lambda)}\right)\right\} + 2\sum_\lambda tr\left\{\Lambda_+(p_-)L_1^{(\lambda)}\Lambda_-(p_+)\left(S_{1R}^{(\lambda)}+S_{2R}^{(\lambda)}\right)\right\} \\ &\quad + \sum_\lambda tr\left\{\Lambda_+(p_-)S_1^{(\lambda)}\Lambda_-(p_+)\left(S_{1R}^{(\lambda)}+S_{2R}^{(\lambda)}\right)\right\}\Big] + [\text{subst.}], \end{aligned} \tag{10}$$

where "subst." means the preceding expression with the substitution (9) carried through. The first trace in (10) together with the substituted one just yields the well-known Bethe Heitler cross section, of course. The following results were obtained for the traces:

$$\sum_\lambda \mathrm{tr}\left\{\Lambda_+(p_-) L_1^{(\lambda)} \Lambda_-(p_+) L_{1R}^{(\lambda)}\right\} = -\frac{n_\mu n_\nu}{m^2 (kp_+)^2}\Big[g_{\mu\nu}\left(\tfrac{1}{2} m^2 q^2 - kp_+\, kp_-\right) + + 2m^2 p_-^\mu p_-^\nu + 2k^\mu p_-^\nu\, kp_+\Big] \qquad (11)$$

$$\sum_\lambda \mathrm{tr}\left\{\Lambda_+(p_-) L_1^{(\lambda)} \Lambda_-(p_+) L_{2R}^{(\lambda)}\right\} = -\frac{n_\mu n_\nu}{m^2\, kp_+\, kp_-}\Big[g_{\mu\nu}\frac{q^2}{2}\left(m^2 - \frac{q^2}{2} - kp_+ - kp_-\right) - - k^\mu k^\nu\left(\frac{q^2}{2} + kp_+\right) + p_-^\mu p_-^\nu (2m^2 - q^2) + k^\mu p_-^\nu\left(q^2 - 2m^2 + kp_+ - kp_-\right)\Big]$$

$$\sum_\lambda \mathrm{tr}\left\{\Lambda_+(p_-) L_1^{(\lambda)} \Lambda_-(p_+) S_{1R}^{(\lambda)}\right\} = -2\left(\frac{2\lambda}{m^*}\right)^2 \frac{n_\mu n_\nu}{m^2\, kp_+ (m^{*2} - m^2 + 2kp_+)}\Big[g_{\mu\nu}\Big(m^2 kp_+ \cdot \cdot\left(-\frac{q^2}{2} - kp_+ - kp_-\right) - mm^*(kp_+ + kp_-)\left(\frac{q^2}{2} + 2kp_+\right) + mm^*\frac{q^2}{2} kp_- + 2kp_-(kp_+)^2\Big) + p_-^\mu p_-^\nu (kp_+ + kp_-)(m^2 - mm^* + 2kp_+) + k^\mu p_-^\nu\left(\frac{q^2}{2} - kp_+\right)(m^2 - mm^* + 2kp_+)\Big]$$

$$\sum_\lambda \mathrm{tr}\left\{\Lambda_+(p_-) L_1^{(\lambda)} \Lambda_-(p_+) S_{2R}^{(\lambda)}\right\} = -2\left(\frac{2\lambda}{m^*}\right)^2 \frac{n_\mu n_\nu}{m^2\, kp_+ (m^{*2} - m^2 + 2kp_-)}\Big[g_{\mu\nu}\Big(m^2 \cdot \cdot\left(-\frac{q^2}{2} kp_+ + (kp_-)^2 + kp_+\, kp_-\right) - mm^*\frac{q^2}{2} kp_+ - 2kp_+ kp_-\left(\frac{q^2}{2} + kp_+ + kp_-\right)\Big) + k^\mu k^\nu\left(m^2 q^2 - 2\left(\frac{q^2}{2} + kp_+\right)^2\right) + p_-^\mu p_-^\nu\Big((m^2 - mm^*)(kp_+ + kp_-) - - 2kp_+\left(\frac{q^2}{2} + kp_+ + kp_-\right) + q^2 kp_-\Big) + k^\mu p_-^\nu\Big((m^2 - mm^*)\left(\frac{q^2}{2} - kp_+\right) - 2m^2 q^2 - - q^2 kp_- + 2\left(\frac{q^2}{2} + kp_+\right)^2 + 2kp_+\left(\frac{q^2}{2} + kp_+ + kp_-\right)\Big)\Big]$$

$$\sum_\lambda \mathrm{tr}\left\{\Lambda_+(p_-) S_1^{(\lambda)} \Lambda_-(p_+) S_{1R}^{(\lambda)}\right\} = 4\left(\frac{2\lambda}{m^*}\right)^4 \frac{kp_+\, n_\mu n_\nu}{m^2 (m^{*2} - m^2 + 2kp_+)^2}\Big[g_{\mu\nu}\, kp_+ \cdot \cdot\Big(m^2(q^2 - 2kp_+ - 2kp_-) + m^{*2}(q^2 + 2kp_+ + 2kp_-) + 2mm^* q^2 + + 4kp_+\, kp_-\Big) + 2k^\mu p_-^\nu q^2 (m^{*2} - m^2 + 2kp_+) - 4p_-^\mu p_-^\nu q^2 kp_+\Big]$$

$$\sum_{\lambda} tr\left(\Lambda_+(p_-)S_1^{(\lambda)}\Lambda_-(p_+)S_{2R}^{(\lambda)}\right) = 4\left(\frac{2\lambda}{m^*}\right)^4 \frac{n_\mu n_\nu}{m^2(m^{*2}-m^2+2kp_+)(m^{*2}-m^2+2kp_-)} \cdot$$

$$\cdot\Big[g_{\mu\nu}(m^*+m)^2\left(kp_+ kp_-(2kp_+ + 2kp_- + q^2) - m^2(kp_+ + kp_-)^2\right) + k^\mu k^\nu\Big((m+m^*)^2 \cdot$$

$$\cdot\, q^2\left(\frac{q^2}{2} + kp_+ - m^2\right) + 4mm^*(kp_+)^2\Big) + p_-^\mu p_-^\nu\, 4mm^*(kp_+ + kp_-)^2 +$$

$$+\, k^\mu p_-^\nu\left((m+m^*)^2 q^2(kp_- - kp_+) - 8mm^*\, kp_+(kp_+ + kp_-)\right)\Big]$$

We further note the following kinematical relations, giving kp_-, kp_+ and q^2 and the fourmomentum of the virtual fermion Q_F^2 in terms of the energy k^0 of the incoming photon and the angles of the electron and the positron defined in Fig. 2, for the case of equal energy of the electron and the positron (neglecting $\frac{m^2}{k^{02}}$ compared with 1):

$$\begin{aligned}
p_-^0 &= p_+^0 = \tfrac{1}{2}\, k^0 \\
k\cdot p_- &\cong k^{02}\sin^2\vartheta_-/2 + m^2\cos\vartheta_- \\
k\cdot p_+ &\cong k^{02}\sin^2\frac{\vartheta_+}{2} + m^2\cos\vartheta_+ \\
p_+\cdot p_- &\cong \frac{k^{02}}{2}\left(\sin^2\frac{\vartheta_+ + \vartheta_-}{2} - \sin^2\frac{\varphi}{2}\sin\vartheta_+\sin\vartheta_-\right) + \\
&\quad + m^2\left(\cos(\vartheta_+ + \vartheta_-) + 2\sin^2\frac{\varphi}{2}\sin\vartheta_+\sin\vartheta_-\right) \\
q^2 &= 2\left(m^2 + p_+\cdot p_- - k\cdot p_- - k\cdot p_+\right) \\
Q_F^2 &= m^2 - 2k\cdot p_- = m^2 - 2k\cdot p_+
\end{aligned} \qquad (12)$$

These realtions together with (2),(10) and (11) yield the cross section for production of pairs with equal energy of the electron and the positron.

3. Cross Section for the Production of the e* in Electron Proton Scattering

In inelastic electron proton collisions the e* can be produced via one photon exchange, subsequently decaying into electron and photon. The cross section was calculated+) according to the diagram of Fig.3, in which the coupling on the electron side is again given by (1). Thus we neglect any form factor of the e*, whereby the cross section may be somwhat overestimated.

+) The cross section is also given in ref. 4

It is given by

$$\frac{d\sigma}{d\Omega^*} = \frac{\lambda^2\alpha^2}{m^{*2}} \; \frac{k^*}{q^4 E_o M\left(E_o + M - \frac{E_o E^*}{k^*}\cos\vartheta^*\right)} \cdot \Big((F_1+F_2)^2 \cdot \tag{13}$$
$$\cdot \left(q^6 + m^{*2} q^4 - 2\, m^{*4} q^2\right) - \left(F_1^2 - \frac{q^2}{4M^2} F_2^2\right)\Big(q^6 +$$
$$+ q^4\left(4W^2 - 4M^2 - m^{*2}\right) + 4q^2\left((W^2-M^2)^2 - m^{*2} W^2\right) + 4m^{*4} M^2\Big)\Big)$$

where

M = mass of the proton,

E_o = initial energy of the electron in the laboratory,

E^* = energy of the e* in the laboratory,

k^* = $\sqrt{E^{*2} - m^{*2}}$

W = $M^2 + 2ME_o$ = total energy in the CMS,

q^2 = $2M(E^* - E_o)$ = momentum transfer to the proton,

F_1 = $F_1(q^2)$, $F_2 = F_2(q^2)$ are the Dirac and Pauli formfactors of the proton with $F_1(0) = 1$, $F_2(0) = 1,79$. The numerical values of the cross section given in ref.3 have been calculated using the form factor fit of ref. 5.

4. Numerical Results and Conclusions

The expressions obtained for the cross section were evaluated numerically for almost symmetric pairs on the IBM computer of DESY and the ratio R of the cross section with the heavy electron and the Bethe Heitler cross section was computed for a set of values of m* and λ. Because of the large dip of the cross section for symmetric electron positron pairs an integration over the positron angles over a small solid angle was performed. The result not depending very sensitively on the intervals chosen, we integrated the cross section over the intervals $\Delta\varphi = 8^\circ$ and $\Delta\vartheta = 0{,}6^\circ$ which roughly agree with the experimental values [3] at $\vartheta = 6^\circ$. An integration over a small energy interval was carried through for one pair of values of λ and m* and did not bring significant changes in R, and a further integration over the electron angles is not necessary either. The results obtained for the ratio R as a function of the fourmomentum Q_F of the virtual fermion for three values of m* and a few values of λ may be seen in table 1.

The experimental values of R[2] are smaller than 1 for values of Q_F smaller than about 200 MeV. We assumed that the absolute normalization in the experiment was wrong by a factor $\frac{2}{3}$ (independent of Q_F) and thus the experimental values of ref. 2) were multiplied by $\frac{3}{2}$.
The values thus obtained may also be found in table 1.
In Fig. 4 a graphical representation is given of the theoretical and experimental values of R from table 1. The following results may be observed:

1) Values of λ between 0,1 and 0,15 for $m^* = 0{,}12$ GeV and λ between 1,2 and 1,6 for $m^* = 0{,}9$ GeV give rough agreement with the experiment. The results obtained for λ for other values of m^* in the range between 0,12 GeV and 1,5 GeV may be found in table 2.

2) Details of the data - though these may be considered not being very significant because of large experimental uncertainties - are not so well reproduced by the theory:
   a) the experimental values of R roughly depend linearly on Q_F^2 whereas the theoretical values - due to the magnetic coupling of the e^* - go up with a higher power of Q_F^2, if m^* is large.
   b) The experimental values of R for fixed Q_F^2 increase with the photon energy (i.e. with decreasing angle), a tendency being also present in the theory, but to an almost negligible extent.

3) The upper limit of λ given by e^* production experiments [3,4] may be seen in table 3. The upper limits given in the mass ranges $120 \leq m^* \leq 500$ MeV and $500 \leq m^* \leq 1000$ MeV are by a factor less than $\frac{1}{2}$ and less than $\frac{1}{10}$ respectively below the lower limits necessary for an explanation of the pair production experiment. Thus we would conclude that the width of an excited electron, if it exists within this mass region is too small to give a considerable effect on the pair production experiment.

Acknowledgement

The authors would like to thank Dr. Hans Joos for suggesting these calculations and for discussions.

Literature

1.) F.E. Low, Phys. Rev. Lett. 14, 238 (1965)

2.) R.B. Blumenthal, D.C. Ehn, W.L. Faissler, P.M. Joseph, L.J. Lanzerotti, F.M. Pipkin, D.G. Stairs, Phys. Rev. Lett. 14, 660 (1965)

R.B. Blumenthal, Thesis, Harvard University 1965

3.) H.J. Behrend, F.W. Brasse, J. Engler, S. Galster, E. Ganßauge, G. Hartwig, H. Hultschig, H. Schopper, DESY-Bericht Nr. 65/9 (1965)

4.) G. Bétourné, H. Nguyen Ngoc, J. Perez y Jorba, J. Tran Thanh, Van, Phys. Lett. 17, 70 (1965)

5.) J.R. Dunning jr., K.W. Chen, A.A. Cone, G. Hartwig, N.F. Ramsay, Phys. Rev. Lett. 13, 631 (1965).

ϑ	$\sqrt{-Q_F^2}$ [MeV]	$-Q_F^2$ 10^{-4} [MeV^2]	R $\lambda = 0{,}04$	R $\lambda = 0{,}09$	R $\lambda = 0{,}125$		$-Q_F^2 \cdot 10^{-4}$ [MeV^2]	R_{exp}
4,80°	59	0,4	1,000	1,003	1,005	4,75°	0,35	0,93 ± 0,06
	118	1,4	1,005	1,030	1,061		1,37	1,16 ± 0,06
	178	3,2	1,019	1,100	1,204		3,10	1,28 ± 0,06
	237	5,6	1,039	1,213	1,446		5,48	1,78 ± 0,06
	266	7,1	1,052	1,287	1,609		6,97	1,62 ± 0,23
	296	8,8	1,066	1,372	1,801		8,58	2,25 ± 0,21
6,15°	76	0,6	1,001	1,006	1,012	6,26°		
	152	2,3	1,011	1,061	1,123		2,37	1,13 ± 0,14
	228	5,2	1,034	1,183	1,382		5,38	1,41 ± 0,14
	303	9,2	1,067	1,378	1,817		9,55	1,82 ± 0,14
	341	11,7	1,087	1,506	2,112		12,04	2,01 ± 0,15
	379	14,4	1,112	1,656	2,468		14,90	2,55 ± 0,35
7,50°	92	0,9	1,002	1,011	1,022	7,50°		
	185	3,4	1,018	1,096	1,198		3,42	1,71 ± 0,20
	277	7,7	1,050	1,277	1,592		7,67	1,95 ± 0,86
	370	13,7	1,097	1,565	2,261			
	416	17,3	1,126	1,758	2,727		17,34	2,25 ± 0,32

Table 1a $m^* = 120$ MeV
Ratio $R = d\sigma$ (Bethe-Heitler + heavy electron)/$d\sigma$(Bethe-Heitler) for symmetric pair production.
Experimental values of R from ref. 2 after multiplication with 1.5.

ϑ	$\sqrt{-Q_F^2}$ [MeV]	$-Q_F^2 \cdot 10^{-4}$ $[\mathrm{MeV}^2]$	R $\lambda = 0,5$	R $\lambda = 0,65$	R $\lambda = 0,75$	ϑ	$-Q_F^2 \cdot 10^{-4}$ $[\mathrm{MeV}^2]$	R_{exp}
$4,80^\circ$	59	0,4	1,000	1,000	1,001	$4,75^\circ$	0,35	$0,93 \pm 0,06$
	118	1,4	1,006	1,010	1,015		1,37	$1,16 \pm 0,06$
	178	3,2	1,032	1,062	1,090		3,10	$1,28 \pm 0,06$
	237	5,6	1,108	1,218	1,329		5,48	$1,78 \pm 0,06$
	266	7,1	1,176	1,364	1,558		6,97	$1,62 \pm 0,23$
	296	8,8	1,281	1,575	1,890		8,58	$2,25 \pm 0,21$
$6,15^\circ$	76	0,6	1,001	1,001	1,001	$6,26^\circ$		
	152	2,3	1,015	1,028	1,041		2,37	$1,13 \pm 0,14$
	228	5,2	1,086	1,173	1,260		5,38	$1,41 \pm 0,14$
	303	9,2	1,285	1,608	1,946		9,55	$1,82 \pm 0,14$
	341	11,7	1,462	2,008	2,587		12,04	$2,01 \pm 0,15$
	379	14,4	1,706	2,573	3,504		14,90	$2,55 \pm 0,35$
$7,50^\circ$	92	0,9	1,001	1,002	1,003	$7,50^\circ$		
	185	3,4	1,031	1,061	1,090		3,42	$1,71 \pm 0,20$
	277	7,7	1,179	1,375	1,579		7,67	$1,95 \pm 0,86$
	370	13,7	1,584	2,298	3,063			
	416	17,3	1,935	3,122	4,411		17,34	$2,25 \pm 0,32$

<u>Table 1b</u> $m^* = 500$ MeV

ϑ	$\sqrt{-Q_F^2}$ [MeV]	$-Q_F^2 \cdot 10^{-4}$ [MeV^2]	R $\lambda = 1,2$	R $\lambda = 1,45$	R $\lambda = 1,6$	ϑ	$-Q_F^2 \cdot 10^{-4}$ [MeV^2]	R_{exp}
4,80°	59	0,4	1,000	1,000	1,000	4,75°	0,35	0,93 ± 0,06
	118	1,4	1,003	1,005	1,007		1,37	1,16 ± 0,06
	178	3,2	1,022	1,037	1,049		3,10	1,28 ± 0,06
	237	5,6	1,085	1,150	1,204		5,48	1,78 ± 0,06
	266	7,1	1,150	1,269	1,370		6,97	1,62 ± 0,23
	296	8,8	1,249	1,455	1,631		8,58	2,25 ± 0,21
6,15°	76	0,6	1,000	1,000	1,000	6,26°		
	152	2,3	1,009	1,015	1,020		2,37	1,13 ± 0,14
	228	5,2	1,066	1,115	1,157		5,38	1,41 ± 0,14
	303	9,2	1,266	1,489	1,680		9,55	1,82 ± 0,14
	341	11,7	1,473	1,885	2,241		12,04	2,01 ± 0,15
	379	14,4	1,793	2,505	3,125		14,90	2,55 ± 0,35
7,50°	92	0,9	1,000	1,000	1,001	7,50°		
	185	3,4	1,021	1,036	1,048		3,42	1,71 ± 0,20
	277	7,7	1,155	1,282	1,391		7,67	1,95 ± 0,86
	370	13,7	1,641	2,215	2,715			
	416	17,3	2,142	3,199	4,124		17,34	2,25 ± 0,32

Table 1c $m^* = 900$ MeV

m* [GeV]	λ
0,12	0,1 $<$ λ $<$ 0,15
0,2	0,15 $<$ λ $<$ 0,3
0,4	0,4 $<$ λ $<$ 0,6
0,5	0,6 $<$ λ $<$ 0,8
0,7	0,9 $<$ λ $<$ 1,2
0,9	1,2 $<$ λ $<$ 1,6
1,1	1,5 $<$ λ $<$ 2,3
1,5	2,5 $<$ λ $<$ 3,4

Table 2. Range of the coupling constant λ suitable for an explanation of pair production as a function of the mass m* of the heavy electron.

ORSAY

m* [MeV]	$\frac{1}{\lambda^2} \geqq$	$\lambda \leqq$
120	600	0,041
150	880	0,034
180	650	0,039
210	600	0,041
240	5.000	0,014
255	2.400	0,021
278	1.300	0,028
304	700	0,038
330	400	0,050
359	210	0,069
391	110	0,095
424	80	0,110
456	55	0,14
493	45	0,15
533	45	0,15
571	45	0,15

DESY

m* [MeV]	$\frac{1}{\lambda^2} \geqq$	$\lambda \leqq$
500	4.900	0,014
600	4.900	0,014
700	4.400	0,015
800	4.000	0,016
900	3.600	0,017
1.000	1.600	0,025

Table 3 Upper limits of λ from the measurements of references 4 (Orsay) and 3 (DESY).

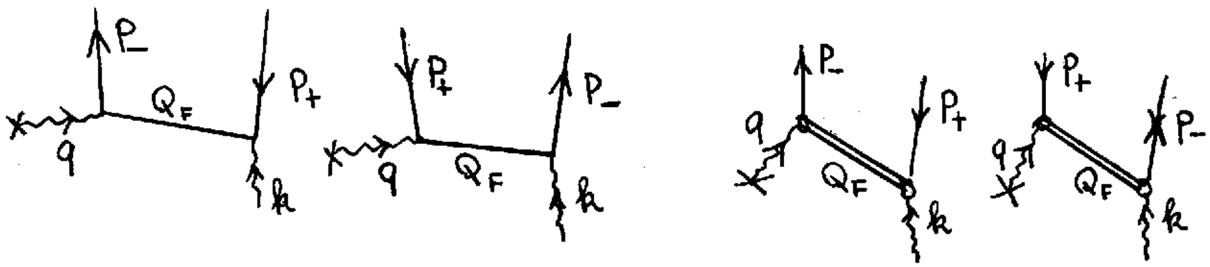

<u>Fig. 1</u> Feynman diagrams for pair production. The double line represents the heavy electron with the coupling $\lambda \frac{e}{m^*} \sigma_{\mu\nu} F_{\mu\nu}$

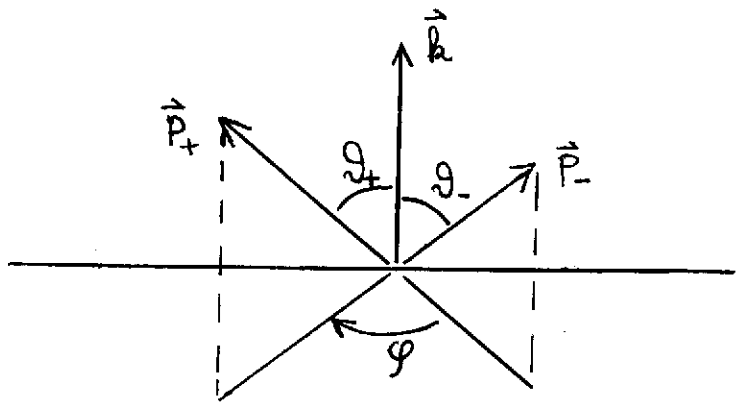

<u>Fig. 2</u> Definition of the angles used.

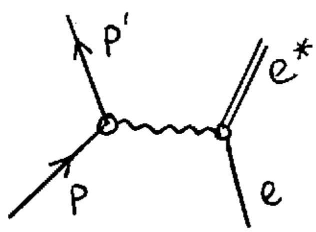

<u>Fig. 3</u> Feynman diagram for e* - production

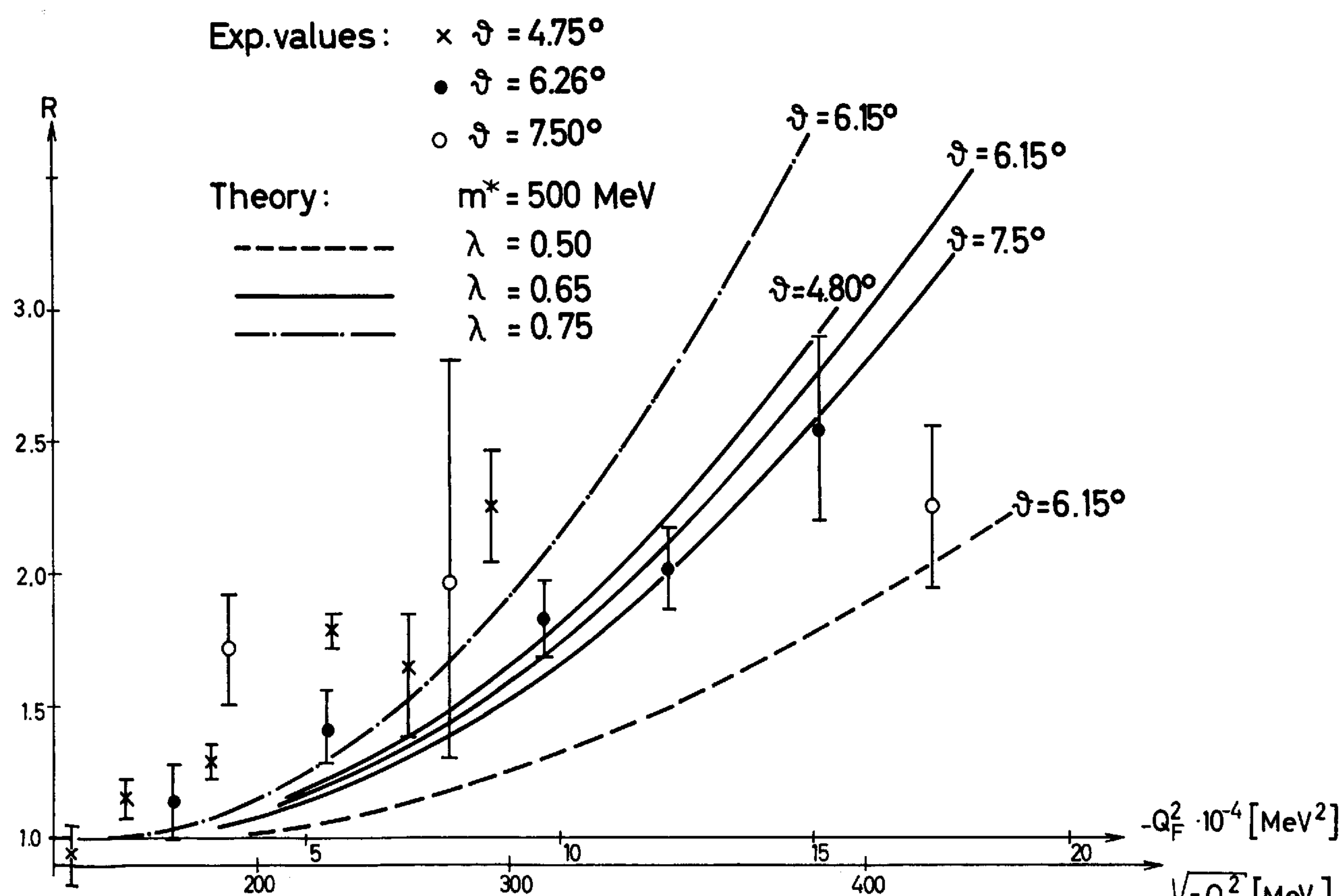

Fig.4b $m^* = 500$ MeV

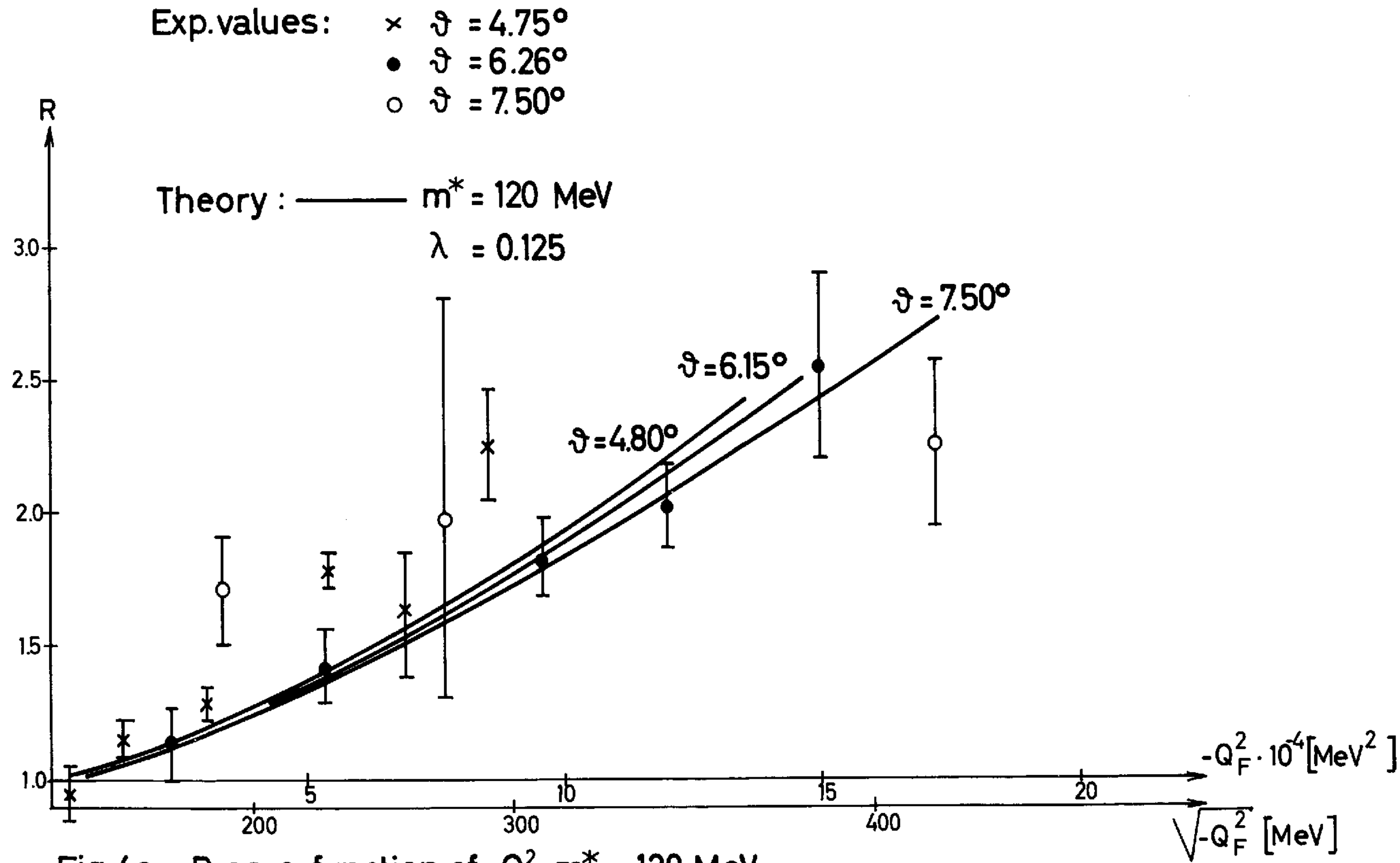

Fig. 4a: R as a function of Q_F^2; $m^* = 120$ MeV